Jiagang Wu

Advances in Lead-Free Piezoelectric Materials

Springer

Advances in Lead-Free Piezoelectric Materials

Jiagang Wu

Advances in Lead-Free Piezoelectric Materials

Springer

Jiagang Wu
Department of Materials Science
Sichuan University
Chengdu, Sichuan, China

ISBN 978-981-10-8997-8 ISBN 978-981-10-8998-5 (eBook)
https://doi.org/10.1007/978-981-10-8998-5

Library of Congress Control Number: 2018947874

This Springer imprint is published by the registered company Springer Nature Singapore Pte Ltd.
The registered company address is: 152 Beach Road, #21-01/04 Gateway East, Singapore 189721, Singapore

Foreword

Piezoelectric materials have been widely used in industry as transducers, sensors, actuators, etc. In recent decades, $Pb(Zr,Ti)O_3$, also called PZT-based materials, have dominated as the piezoelectric driving elements in these high-performance piezoelectric devices. Although PZT-based materials have excellent physical properties, a high content of lead ($\sim$60 wt%) inevitably causes environmental issues during the preparation and disposal processes. Such environmental issues have led to the prohibition of lead usage by laws and regulations. Thus, lead-free piezoelectric materials have attracted ever-increasing attention.

Since 2000, significant progress has been made in the research and development of lead-free piezoelectric materials, with their physical properties being comparable to those of PZT. For perovskite-structured ferroelectrics, the piezoelectric properties have been dramatically improved by the construction of phase boundaries. For example, the piezoelectric constants of $BaTiO_3$ and $(K,Na)NbO_3$-based ceramics can match or exceed those for some PZT ceramics. $BiFeO_3$ solid solutions with other ABO_3 can simultaneously realize a high Curie temperature and large piezoelectricity that are comparable to that of $BiScO_3$–$PbTiO_3$. Furthermore, a large unipolar strain (0.7%) was observed in polycrystalline $(Bi_{0.5}Na_{0.5})TiO_3$-based lead-free piezoelectric materials and is first superior to those of some PZT-based ceramics. In addition, bismuth layer-structured ferroelectrics have been good candidates for lead-free high-temperature piezoelectric devices. As a result, we believe that the advances in lead-free piezoelectric materials can promote far-reaching and practical applications with a complete replacement for lead-based piezoelectric materials in the future.

This book—written by Dr. Jiagang Wu, who has been working on piezoelectric materials—consists of nine chapters. The first chapter provides the historical evolution of the field of piezoelectrics, covering basic knowledge of the piezoelectric effects, and dominant factors affecting the piezoelectric effect, as well as a brief summarization of the development of lead-free piezoelectrics. The second chapter introduces the preparation techniques of lead-free piezoelectrics and the characterization methods of their electrical properties and microstructure. The following five (third to seventh) chapters review the developments of important lead-free piezoelectric materials, such as barium titanate, bismuth sodium titanate, bismuth

ferrite, potassium sodium niobate, and the bismuth layer-structured ferroelectric family. The fundamentals and properties of these lead-free ferroelectric families are discussed, and in particular, the principles and design rules of phase boundaries are illustrated for the perovskite family. The eighth chapter evaluates the properties of lead-free piezoelectric materials in comparison with those of lead-based piezoelectrics. Finally, the last chapter addresses an overview of the applications of lead-free piezoelectric materials and evaluates the advantages and disadvantages of lead-free electronic devices. Thus, this book provides a comprehensive review and evaluation of lead-free piezoelectric materials. Some critical issues for the development of lead-free piezoelectric materials are also addressed. This book covers most of the fundamentals in the field of lead-free piezoelectric materials, providing a historical perspective, the present status, and future directions. The contents are very useful to researchers and engineers in this field.

Beijing, China

Cewen Nan
Tsinghua University

Contents

Chapter 1
Historical Introduction

Abstract Piezoelectric materials are currently used in many electronic devices because of excellent properties. Here, we briefly introduce the historical evolution of piezoelectric effect and also emphasize the importance of some factors (e.g., phase transition, microstructure, poling behavior) on the piezoelectricity of a material. Due to the toxicity of Pb in lead-based piezoelectrics, lots of attention has been given to lead-free piezoelectric materials, especially the use of phase boundaries. Importantly, we summarize the development of lead-free piezoelectrics, and some great advances have been demonstrated. We believe that the advances in lead-free piezoelectric materials will promote the practical applications.

1.1 Piezoelectric Effect

Piezoelectricity is usually defined as the electric charge accumulating in certain solid materials when the mechanical stress was applied [1]. In 1880, the direct piezoelectricity was firstly discovered in the single-crystal quartz by the French physicists of Jacques and Pierre Curie, and then the converse piezoelectric effect was also observed by Gabriel Lippmann in 1881. It was found that the single-crystal quartz as piezoelectric materials can induce electrical charge/voltage under the pressure, and thus "piezoelectricity" presents "pressure electricity" because of the root of the word 'piezo' means 'pressure' in Greek. These findings help understanding the fundamental role of the symmetry in the laws of physics.

Piezoelectric effect is a reversible process, which can be thought as a linear electromechanical interaction between the mechanical and the electrical state of a material without inversion symmetry [2]. Two categories can be defined in piezoelectric effect: direct piezoelectric effect and reverse piezoelectric effect (Fig. 1.1). Direct piezoelectric effect is the internal generation of electrical charge under an applied mechanical force, and the reverse piezoelectric effect can be defined as the internal generation of mechanical strain resulting from electric fields.

J. Wu, *Advances in Lead-Free Piezoelectric Materials*,
https://doi.org/10.1007/978-981-10-8998-5_1

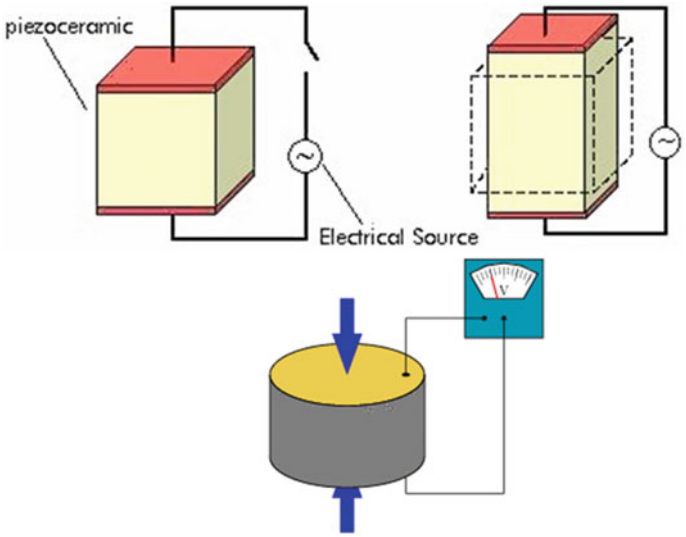

Fig. 1.1 Sketch images for piezoelectric effects

Piezoelectric materials endure the historical episodes in the sequence of quartz, Rochelle salt, barium titanate, $Pb(Zr,Ti)O_3$, lithium niobate/tantalate, relaxor ferroelectrics, PVDF, Pb-free piezoelectrics, and composites. Piezoelectric ceramics were first put to practical applications in around 1950 [3] and have been widely used in industries since then. Currently, most of applied piezoelectric materials are still based on lead zirconate titanate [$Pb(Zr,Ti)O_3$, PZT]. Recently, lead-free piezoelectric materials have been quickly developed due to the environmental friendliness, and especially some physical properties can be comparable to the lead-based ones by the efforts of decades.

1.2 Dominant Factors to Piezoelectric Effect

Piezoelectric effect of a material can be dominated by some factors, such as phase structure, domain structure, preparation technique, poling condition, etc. In particular, it is well known that high piezoelectricity can be often observed in relation with high instability of crystal structure or domain configuration, and the poling condition also strongly affects their piezoelectric properties. Therefore, we eminently introduced such three aspects (phase transition, poling behaviour, and domain configuration), and especially the evolution of phase structure in lead-based and lead-free materials will be importantly emphasized.

1.2.1 Phase Transitions

Phase transitions in perovskite materials are often associated with a variation in ferroelectric/piezoelectric properties. The phase transition points of ferro/piezoelectric materials can be changed by some factors (i.e., composition, temperature, electric field or stress), and then the flattening of the free-energy profile can always result in the phase instability [4–6]. More importantly, the formation of phase boundaries can lead to the enhancement of electrical properties of the ferro/piezoelectrics [7]. In this part, we summarized phase transitions reported for lead-based or lead-free perovskite-type compounds, where a ferroelectric phase transition was involved.

1.2.1.1 Lead-Based Materials

In the past, the lead-based materials have dominated the whole development and applications of piezoelectric electronic devices because of superior properties. Lead-based piezoelectric materials mainly include normal and relaxor ferroelectrics, where $(1 - x)PbZrO_3$–$xPbTiO_3$ and relaxor-$PbTiO_3$ were respectively considered as the outstanding candidates of normal and relaxor ones. In addition, the current phase boundaries of lead-free materials are almost borrowing ideas from the lead-based ones, especially the morphotropic phase boundary (MPB) concept of PZT. Here, we briefly illuminated the development of phase transitions in the lead-based materials by addressing three typical samples of $(1 - x)PbZrO_3$–$xPbTiO_3$, $(1 - x)Pb(Zn_{1/3}Nb_{2/3})O_3$–$xPbTiO_3$, and $(1 - x)BiScO_3$–$xPbTiO_3$, and the relationship between phase boundary and electrical properties was addressed.

$(1 - x)PbZrO_3$–$xPbTiO_3$

The solid solutions consisting of $PbZrO_3$ and $PbTiO_3$ [$(1 - x)PbZrO_3$–$xPbTiO_3$] were firstly investigated by G. Shirane and co-workers in 1952 [8], the phase diagram was established by E. Sawaguchi in 1953 [9], and the discovery of its superior piezoelectricity was reported by Bernard Jaffe in 1954 (Fig. 1.2a) [10, 11]. As we know, PZT has a perovskite structure, and two important factors determine its superior piezoelectricity, including Pb-induced and MPB. In addition, their electrical properties can be easily modified by the composition design, and "hard" and "soft" PZT can be realized by doping different compositions. For example, the additions of low valance cations (e.g., K^+ for Pb^{2+}, Fe^{3+} for Ti^{4+} or Zr^{4+}) can easily result in the formation of oxygen vacancies and limit the domain wall motion, thus deteriorating the piezoelectric properties. The typical representatives for "hard" PZT are PZT-4 and PZT-8. Soft PZT can be attained by doping high valance cations (La^{3+} for Pb^{2+}, Ta^{5+} and Nb^{5+} for Ti^{4+} or Zr^{4+}), as represented by PZT-5A and PZT-5H. These tailored properties can well meet the practical applications. As a result, the composition-induced ferroelectric phase transition is generally employed to enhance the piezoelectric response of lead-based systems, that is, the

contribution of polarization rotation to piezoelectric properties can be greatly enhanced by selecting proper ferroelectric solid solutions with MPB.

In the past decades, several typical materials have shown that the formation of multiphase coexistence can promote the piezoelectric properties of a ferro/piezoelectric material [10–12]. Among these materials, considerable attentions have been given to perovskite piezoelectrics because of their outstanding properties, which were studied for various practical applications including transducers, sensors, actuators, energy harvesting devices, multilayer ceramic capacitors, photovoltaic and electrocaloric devices, and infrared sensors. $Pb(Zr_xTi_{1-x})O_3$ (PZT) is always thought as the most successful piezoelectric materials in electronic devices because of the involvement of large piezoelectricity (Fig. 1.3) [11]. The enhancement of electrical properties in PZT commonly originates from a nearly temperature-independent MPB by modifying the Zr/Ti ratios (Fig. 1.2a) [10]. Namely, when the compositions are in the vicinity of MPB, the increased number

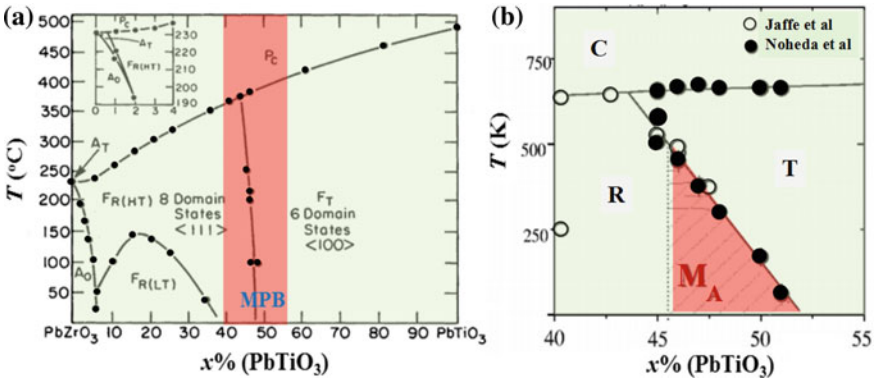

Fig. 1.2 **a** Phase diagram of $(1 - x)PbZrO_3$–$xPbTiO_3$ reported by Jaffe et al. [11] and **b** revised phase diagram for PZT in the vicinity of the MPB [14]. Reprinted with permission from Ref. [11]. Copyright © 1971, Elsevier. Reprinted with permission from Ref. [14]. Copyright © 2001, AIP Publishing LLC

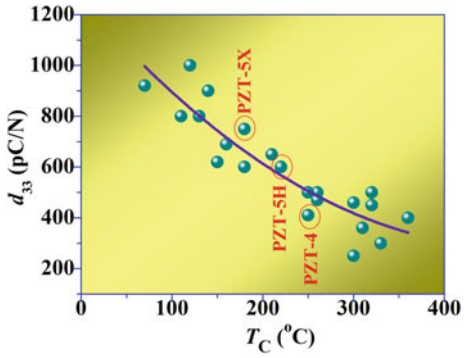

Fig. 1.3 d_{33} versus T_C of PZT materials

of thermo dynamically equivalent states can substantially improve the alignment of randomly oriented ferroelectric domains, allowing optimum polarization under an applied electric field.

Previously, it was thought that the tetragonal and rhombohedral phases were involved into the PZT with MPB. The phase boundary between rhombohedral and tetragonal phases is vertically elongated around the compositions with Zr/Ti = 53/47, and the phase structure is very sensitive to the variations of Zr/Ti ratio near MPB [10]. However, the opinions about MPB in PZT were challenged by some experimental and theoretical methods, and an intermediate phase was thought to coexist in MPB [13, 14]. For example, the monoclinic phase between tetragonal and rhombohedral phases was found in the $PbZr_{1-x}Ti_xO_3$ (x = 0.45–0.5) system using the synchrotron X-ray powder diffraction measurements [15], and moreover, it was also observed that the most plausible space group for the new monoclinic phase belongs to be Cm. In 2001, Noheda et al. and Cox et al. also found that a new phase existed in the phase diagram near the MPB between the rhombohedral and tetragonal phases, as shown in Fig. 1.2b. One can find from Fig. 1.2b that the lower-symmetry phase (monoclinic M_A type) (Cm) is shown in the PZT system with $0.46 < x < 0.52$. Currently, there are still some disputes about the phase structure of PZT with MPB [16–19], and then the further researches are needed with the attempt to clarify the MPB. Anyway, the polarization rotation in the presence of monoclinic phases (Noheda 2002; Noheda and Cox 2006), particularly in the morphotropic phase boundary region, can be generally thought as the main mechanisms of large piezoelectricity along non-polar axes in complex lead-based solid solutions.

$(1 - x)Pb(Zn_{1/3}Nb_{2/3})O_3$–$xPbTiO_3$

The lead-based materials with ultrahigh piezoelectric performance were developed by the thoughts of MPB, which benefited the innovations of actuators, sensors, and ultrasonic transducers. As we know, it was difficult to fabricate the PZT-based single crystals with big size because of the incongruent melting feature of the solid solutions and the refractory zirconate. Therefore, one kind of novel relaxor ferroelectric single crystals [$A(B_1B_2)O_3$–$PbTiO_3$] was invented, where $A(B_1B_2)O_3$ is relaxor ferroelectric and $PbTiO_3$ is normal ferroelectric. Among these relaxor ferroelectrics, $Pb(Zn_{1/3}Nb_{2/3})O_3$ (PZN) was the leading candidates, and then $(1 - x)Pb(Zn_{1/3}Nb_{2/3})O_3$–$xPbTiO_3$ (PZN–xPT) single crystals were considered to be one of the most famous candidates [20–27]. The advance in the fabrication technique of crystal growth has been firstly realized since Park and Shrout reported the high-quality relaxor-$PbTiO_3$ single crystals in 1990s following the earlier work of Kuwata et al. in 1982 [28]. In addition, the large-size relaxor-$PbTiO_3$ can be also attained by the modified Bridgman method [29]. The structure of PZN–xPT crystals mainly depends on the composition (x), where PZN and PT are respectively rhombohedral and tetragonal phases. The large-size PZN–xPT single crystals possessed the phase diagram similar to PZT, and then its electrical properties were enhanced. For example, ultrahigh piezoelectric constant (d_{33} = 1500–2500 pC/N) and electromechanical coupling factors ($k_{33} > 0.9$) can be found in PZN–xPT

(x = 0.28–0.33) single crystals with MPB. Finally, the enhancement of piezoelectricity was also ascribed to the formation of MPB.

Lots of investigations have attempted to understand the origin of giant piezoelectric coefficients in these perovskite oxides [$Pb(Zr_{1-x}Ti_x)O_3$ and $(1-x)Pb(Zn_{1/3}Nb_{2/3})O_3$–$xPbTiO_3$] with MPB [10, 13, 14, 21, 30]. Originally, the MPB is considered as an almost vertical phase boundary separating the rhombohedral and the tetragonal regions of the phase diagram of these systems (temperature versus x) (Figs. 1.2a and 1.4a). However, the complication of MPB is far from our expectation. Similarity to the complex structure of PZT with MPB, the relaxor ferroelectrics also endured the complicated phase transitions with the variations of chemical compositions, electric field or stress. Here, we illuminated the changes of MPB by choosing the classical sample of $Pb(Zn_{1/3}Nb_{2/3})O_3$–$PbTiO_3$ single crystals. In 1981, J. Kuwata et al. found that morphotropic phase boundary in PZN–xPT single crystals consists of rhombohedral and tetragonal phases (Fig. 1.4a), as confirmed by their dielectric, piezoelectric and pyroelectric properties. Significantly, it was thought that the construction of MPB can result in the anomalously large electromechanical and piezoelectric constants of PZN–xPT [21]. Cox et al. found that a new phase (O) existed in the phase diagram of PZN–xPT

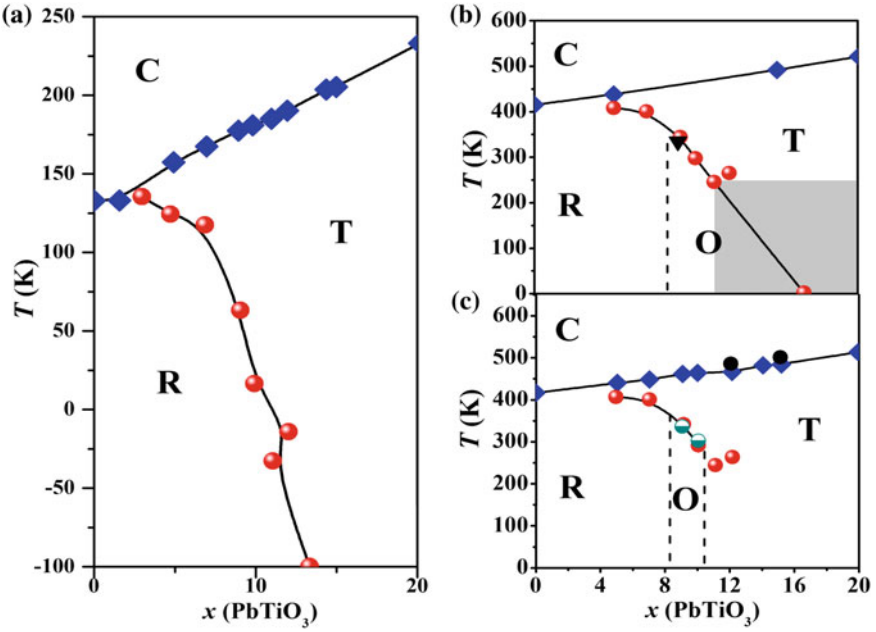

Fig. 1.4 **a** Phase diagram of $(1-x)Pb(Zn_{1/3}Nb_{2/3})O_3$–$xPbTiO_3$system [21], **b** revised phase diagram [14], and **c** updated phase diagram with high concentrations of $10\% < x < 15\%$ [30]. Reprinted with permission from Ref. [21]. Copyright © 1981, Taylor & Francis. Reprinted with permission from Ref. [14]. Copyright © 2001, AIP Publishing LLC. Reprinted with permission from Ref. [30]. Copyright © 2002, The American Physical Society

near the MPB by X-ray investigations (Fig. 1.4b) [14]. In PZN–xPT (x = 0.08) single crystal, an orthorhombic (O) phase can be induced by the application of external electric fields [31, 32]. Especially, with the increase of the applied electric fields, the polarization vector of PZN–xPT crystals firstly obeys the path of R-M_A-T and then shifts to a new path of R-M_A-M_C-T [31]. In addition, the irreversible polarization path for R-M_A-M_C-T was also confirmed by the neutron diffraction [33], and similar polarization path was also found in PZT [34]. By studying the phase structure of PZN–xPT ($10\% < x < 15\%$) using the high-resolution synchrotron X-ray powder diffraction, the low-temperature orthorhombic structure was disappeared for $x > 10\%$ (Fig. 1.4c), confirming the involvement of an orthorhombic phase in only a narrow concentration range (8–11%) [30]. Therefore, the actual phase structure for MPB is still an open question regardless of PZT or relaxor-$PbTiO_3$, but it is sure that such a MPB is responsible for the enhancement of piezoelectric properties.

$(1 - x)BiScO_3$–$xPbTiO_3$

Perovskite PZT has dominated the world markets for piezoelectric materials since its discovery in 1950s, and the enhancement of piezoelectric activity can be observed in MPB due to a high domain orientation during poling process. In addition, the design idea of MPB has been applied in the relaxor $(1 - x)Pb(B_1B_2)O_3$–$xPbTiO_3$ systems, and ultrahigh piezoelectricity can be attained. However, it was also observed that the enhanced performance of commercial lead-based systems generally results in a decreased T_C (Fig. 1.3). In particular, the requirement for actuator and sensor over a broad temperature range is essential in the automotive and aerospace industries [35]. Therefore, it is necessary to develop the piezoelectric materials with large piezoelectricity as well as high Curie temperature. In the past, one kind of ferroelectric materials with high Curie temperature has been developed by the equation of $(1 - x)BiMeO_3$–$xPbTiO_3$ solid solutions (Me=Sc, In, Yb, Fe) [36]. In particular, $(1 - x)BiScO_3$–$xPbTiO_3$(BS–xPT) showed the enhancement of electrical properties (d_{33} = 450 pC/N) together with a high T_C of 450 °C when the compositions approached a MPB (x = 0.64) [28]. According to the phase diagram (Fig. 1.5), there is a nearly linear relationship between T_C and $PbTiO_3$ contents [37]. In addition, the MPB of ferroelectric tetragonal and rhombohedral phases was observed at room temperature, resulting in the enhancement of piezoelectric properties [38]. Recently, a giant unipolar strain of ~0.45% ($T_C \sim$ 425 °C) and a temperature-insensitive piezoelectric effect ($d_{33} \sim$ 520 pC/N) have been observed in $(1 - y)[xBiScO_3$–$(1 - x)PbTiO_3]$–$yBi(Zn_{1/2}Ti_{1/2})O_3$ ceramics (Fig. 1.6), which was assigned to the formation of MPB as well as the optimized chemical compositions [35]. The ceramics possessed a superior d_{33} value with respect to pure BS-PT, and the largest strain can be also found as compared with other lead-based ceramics. Therefore, the comprehensive performance is almost superior to the previously reported results in lead-based materials.

According to the development of lead-based piezoelectric materials, it can be concluded that the concept of MPB benefits the improvement of electrical properties. The composition-induced phase boundaries can put the lead-based

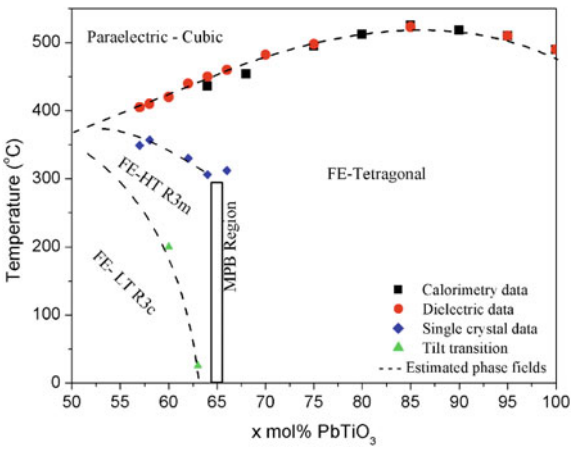

Fig. 1.5 Phase diagram of $(1 - x)BiScO_3$–$xPbTiO_3$ system according to the data collecting from the TEM and single crystal [37]. Reprinted with permission from Ref. [37]. Copyright © 2004, AIP Publishing LLC

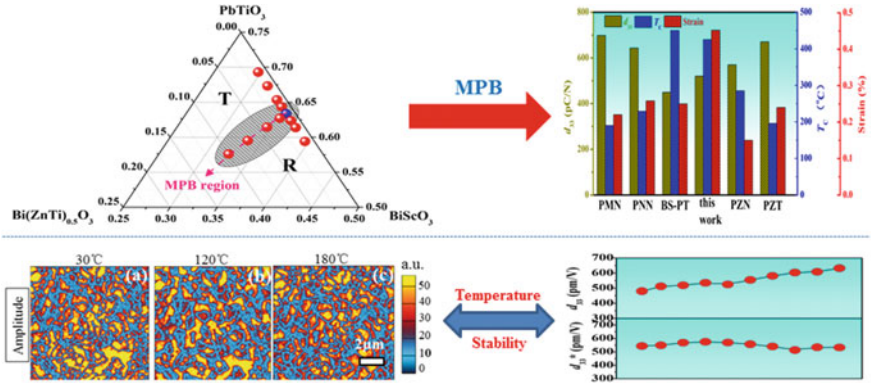

Fig. 1.6 Formation of MPB through optimizing composition makes this ternary system superior to other lead-based piezoceramics. The stable domain structure is mainly responsible for the excellent temperature stability [35]. Reprinted with permission from Ref. [35]. Copyright © 2018, Royal Society of Chemistry

piezoelectric materials into practical applications. More importantly, the designed idea can provide a new road to tailor the properties of lead-free piezoelectric materials.

1.2.1.2 Lead-Free Materials

According to the researches of lead-free piezoelectric materials, the construction of phase boundaries is very effective to promote piezoelectric properties. For example, the d_{33} can be enhanced in $BaTiO_3$ by constructing R-T phase boundary, but a low T_C (<100 °C) is often shown. However, the characteristics of R-T in lead-free materials are obviously different from lead-based ones, where the phase boundaries

of most lead-free materials are often sensitive to both temperature and composition. Although the "real" MPB can be constructed in the $Bi_{0.5}Na_{0.5}TiO_3$-based ceramics, the poor d_{33} and a low T_d seriously limited its practical applications. Recently, the $BiFeO_3$ solid solutions have exhibited a high piezoelectricity due to the formation of phase boundaries, but the high conductivity inevitably affected the applications. Our group recently improved the piezoelectricity of (K,Na)NbO_3-based ceramics by constructing R-T phase boundary, but the temperature sensitivity of d_{33} still needs to be further solved. As a result, it is necessary to illuminate the idea of phase boundaries in lead-free piezoelectric materials, which benefited the further development of electric properties.

$BaTiO_3$

Barium titanate ($BaTiO_3$, BT) was firstly developed as a piezoelectric material, which was extensively studied till now because of high coupling factors, chemical stability, and easy manufacture. Three countries of US, Japan and Russia contributed to the discovery of BT ceramics [39]. Commonly, Barium titanate has three kinds of phase transition temperatures with decreasing temperatures, including T_C (120 °C), $T_{O\text{-}T}$ (0 °C), and $T_{R\text{-}O}$ (−90 °C). As well known, site engineering is an effective way to construct the phase boundaries in BT by moving three kinds of phase transition temperatures, finally improving its electrical properties. In 2009, the lead-free piezoceramic system of $Ba(Ti_{0.8}Zr_{0.2})O_3$–$(Ba_{0.7}Ca_{0.3})TiO_3$ showed a high piezoelectric coefficient of $d_{33} \sim 620$ pC/N by the construction of phase boundaries using the chemical modifications [40], which greatly motivated further investigations of the whole solid solutions containing BT. As shown in the phase diagram of Fig. 1.7a, they thought that a MPB consisted of a tricritical triple point of a cubic paraelectric phase (C), ferroelectric rhombohedral (R) and tetragonal (T) phases according to the temperature dependence of dielectric properties, which was responsible for the high piezoelectricity [40]. However, D. S. Keeble et al.

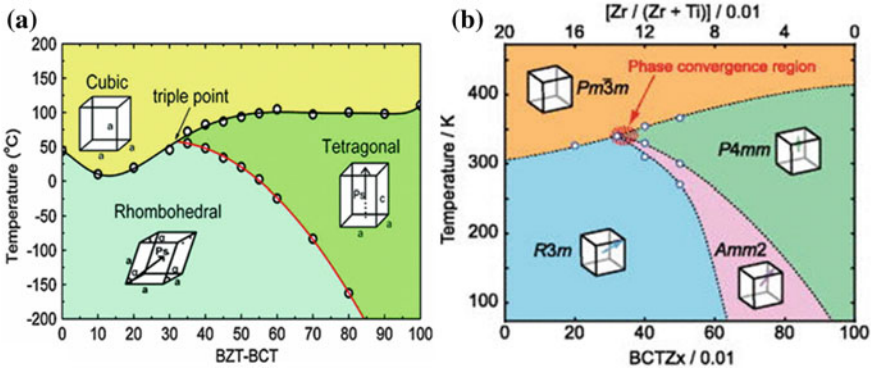

Fig. 1.7 Phase diagram of $Ba(Zr_{0.2}Ti_{0.8})O_3$–$(Ba_{0.7}Ca_{0.3})TiO_3$ system reported by **a** X. B. Ren [40] and **b** Dean S. Keeble [41]. Reprinted with permission from Ref. [40]. Copyright © 2009, The American Physical Society. Reprinted with permission from Ref. [41]. Copyright © 2013, AIP Publishing LLC

studied the phase diagram of $Ba(Ti_{0.8}Zr_{0.2})O_3$–$(Ba_{0.7}Ca_{0.3})TiO_3$ ceramics using the high-resolution synchrotron x-ray powder diffraction, and the intermediate orthorhombic phase bridging T-R can be observed in the same material system (Fig. 1.7b) [41]. Therefore, the polarization rotation between R and T phases through the intermediate phase can result in the strong piezoelectric properties of this work. Although some disputes concerned about the types of phase boundaries, the piezoelectric properties can be always enhanced. The superior piezoelectricity can be revealed in $BaTiO_3$-based ceramics, which is comparable with soft PZT. We have to point out that the material system has the drawback of low Curie temperature (T_C < 130 °C), restricting its application for its temperature stability performance. However, it can be thought as an excellent model system for exploring the physical mechanisms of high-performance Pb-free piezoelectric materials.

$BiFeO_3$

$BiFeO_3$-based material should be considered as a promising material in high-temperature applications due to its high Curie temperature (T_C), and thus lots of investigations have been conducted in recent years [42]. Except for high leakage current, the lack of real MPB seriously hindered the development of BFO materials in terms of ferroelectric and piezoelectric properties. In the past, the composition or strain-induced phase boundaries were observed in BFO materials (thin films or bulks). For example, the strain modulation can drive the formation of phase boundaries on a length scale of tens of nanometers in 85-nm-thick $BiFeO_3$/$LaAlO_3$(001) thin films, and thus huge piezoelectric response can be observed [43]. The structural information about the mixed phases was unveiled by the higher-resolution atomic image, as shown in Fig. 1.8a. It was found that the T phase interspersed between two R phase regions. One can see from Fig. 1.8b that the out-of-plane lattice parameter endured the changes from 4.06 Å (R) to 4.65 Å (T) without the insertion of misfit dislocations, and the in-plane lattice parameter changed slightly from ~3.8 Å (R) to ~3.7 Å (T) because this parameter was

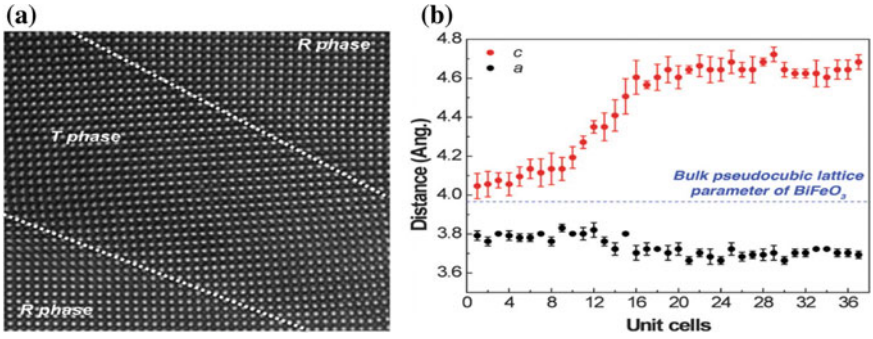

Fig. 1.8 **a** High-resolution TEM image of the boundaries between R and T regions in an 85-nm-thick $BiFeO_3$/$LaAlO_3$(001) thin film. **b** Corresponding in-plane (a, black) and out-of-plane (c, red) lattice parameters [43]. Reprinted with permission from Ref. [43]. Copyright © 2009, The American Association for the Advancement of Science

constrained by the $LaAlO_3$ substrate. In over 10 unit cells, the c/a ratio shifted from 1.07 (R) to 1.27 (T). In addition, density functional calculations were also employed to confirm the coexistence of R and T phases. Therefore, the strain-driven phase changes effectively improved the piezoelectric properties in BFO [43].

As far as the BFO bulks were concerned, ion substitutions cannot induce the formation of effective ferroelectric phase boundaries which can improve its electrical properties, and then a poor d_{33} of <50 pC/N was observed [42]. Although chemical modifications and optimized preparation process were applied, their piezoelectric constant was also difficult to exceed 50 pC/N. However, the solid solutions of BFO with other ABO_3 can construct the phase boundaries (e.g., R-pseudo C, R-T, R-monoclinic), and then the enhancement of piezoelectricity (d_{33} = 100–200 pC/N) can be often attained [42]. Especially, the solid solutions consisting of bismuth ferrite and barium titanate can achieve good piezoelectric properties with high Curie temperature when fabricated with low-temperature sintering followed by a water-quenching process. Recently, the obvious advance in piezoelectricity has been reported in $BiFeO_3$–$BaTiO_3$ (BFO-BTO)-based materials (Fig. 1.9b) [44]. It was found that MPB or PPT can be constructed in BFO-BTO-based materials, and then a large d_{33} of 402 pC/N together with a high T_C of ~454 °C can be shown in $0.67Bi_{1.05}(Fe_{0.97}Ga_{0.03})O_3$–$0.33BaTiO_3$ ceramics (Fig. 1.9a). The d_{33} values of the BFO-BTO-based material system are as high as those of PZT ceramics, and their T_C values are also higher than those of PZT ceramics.

$(K,Na)NbO_3$

Potassium-sodium niobate [$(K,Na)NbO_3$, KNN] materials have been thought as one of the most promising lead-free piezoelectric candidates because of relatively good comprehensive performance [45]. In 2004, a large d_{33} of ~416 pC/N was realized in KNN-based ceramics by RTGG method (Fig. 1.10a, b) [46], which is the first time to attain such high piezoelectricity in KNN materials. Since 2004, lots of

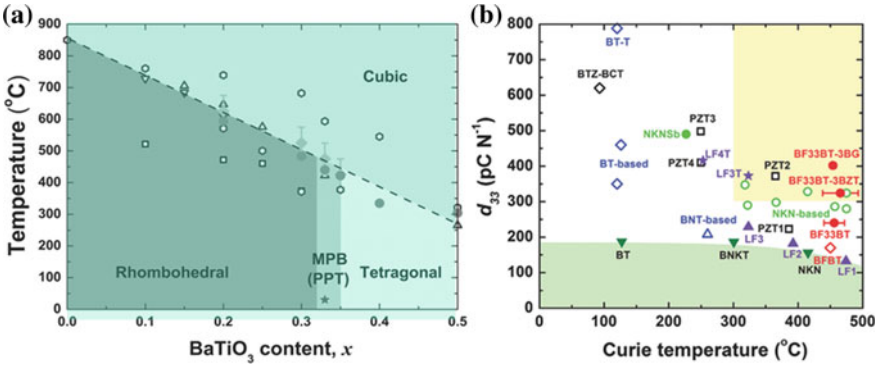

Fig. 1.9 **a** Phase diagram of $0.67Bi_{1.05}FeO_3$–$0.33BaTiO_3$ ceramics. **b** Piezoelectric properties (d_{33}) and Curie temperatures (T_C) of various piezoceramics [44]. Reprinted with permission from Ref. [44]. Copyright © 2015, Wiley

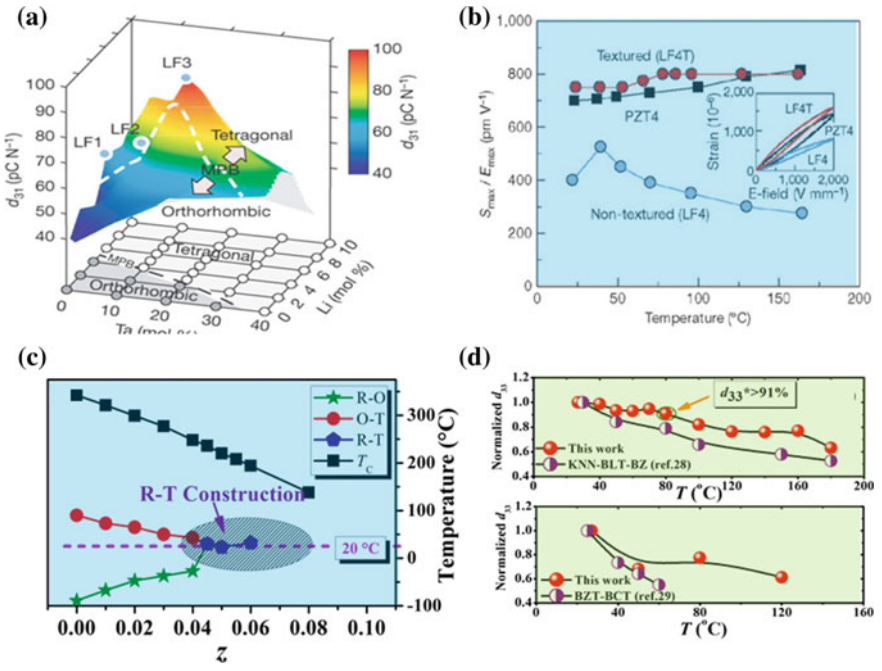

Fig. 1.10 **a** Phase diagrams and **b** temperature stability of strain behavior of the textured and non-textured KNN-based ceramics [46]. **c** Phase diagram and **d** temperature stability of strain and piezoelectricity in $(1-x)(K_{1-y}Na_y)(Nb_{1-z}Sb_z)O_3$–$xBi_{0.5}(Na_{1-w}K_w)_{0.5}HfO_3$ ($x = 0.035$, $y = 0.52$, $z = 0.05$ and $w = 0.18$) ceramics [48]. Reprinted with permission from Ref. [46]. Copyright © 2004, Springer Nature. Reprinted with permission from Ref. [48]. Copyright © 2017, Royal Society of Chemistry

efforts have been given to the KNN-based materials by constructing the O-T phase boundary [45]. For example, a high d_{33} of 320–324 pC/N as well as a good temperature stability were suggested by Jing-Feng Li's group [47]. However, it is difficult to make large breakthrough in piezoelectricity by the formation of O-T phase boundary. Recently, the new phase boundary (R-T) has been constructed in KNN-based ceramics by our group (Fig. 1.10c) [48], and more importantly the big breakthroughs in d_{33} were achieved (Fig. 1.11) [49]. For example, in 2014, we developed the lead-free ceramic materials from potassium-sodium niobate with $d_{33} \sim 490$ pC/N [50], which was firstly found to be superior to the textured KNN-based ceramics as reported by Saito et al. in 2004 [46]. In this work, the new phase boundary (R-T) was employed to promote the piezoelectric properties of KNN-based ceramics. After that, our group attained a series of giant d_{33} (490–570 pC/N) by forming R-T phase boundary using the optimization of chemical compositions (Fig. 1.11) [48–50]. In particular, it was confirmed that such a high d_{33} value can be ascribed to the co-existence of "nano-scale strain domains" (1–2 nm) and R-T phase boundary [49].

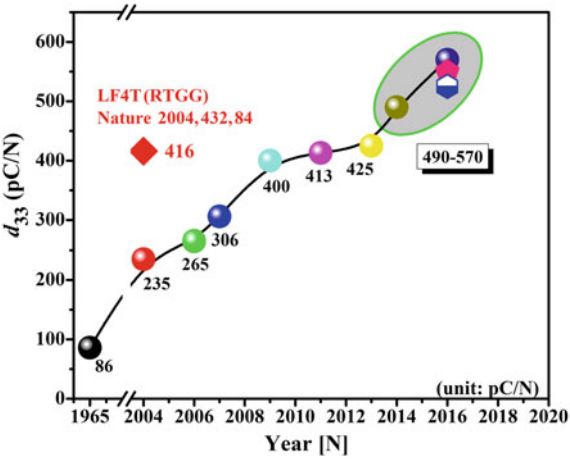

Fig. 1.11 Historical development of piezoelectricity in KNN-based materials [49]. Reprinted with permission from Ref. [49]. Copyright © 2016, Wiley

The temperature stability of electrical properties in piezoelectric materials is very important for industrial applications [45]. Previously, it was thought that d_{33} of KNN-based materials is very sensitive to the surrounding temperature due to the characteristics of PPB [45]. As shown in Fig. 1.10b, there is a poor temperature stability of strain values for the non-textured KNN-based ceramics, and therefore it is necessary to improve the temperature stability of electrical properties for practical applications [48]. In 2017, a new material system of $(1-x)(K_{1-y}Na_y)(Nb_{1-z}Sb_z)O_3$–$xBi_{0.5}(Na_{1-w}K_w)_{0.5}HfO_3$ was developed by us, and the R-T phase boundary can be constructed by the composition modification ($x = 0.035$, $y = 0.52$, $z = 0.05$ and $w = 0.18$) (Fig. 1.10c). Figure 1.10d showed the temperature dependence of normalized inverse piezoelectric coefficient (d^*_{33}) and d_{33} of the ceramics. The d^*_{33} fluctuated less than 10% for 27–80 °C, and a high d^*_{33} (~362 pm/V) still remained even if the temperatures reached 160 °C. In addition, d_{33} remained 77% for ~80 ° C (Fig. 1.10d), indicating the existence of a relatively good temperature stability of d_{33}. Here, the temperature stability of d^*_{33} in $0.92K_{0.5}Na_{0.5}NbO_3$–$0.02Bi_{1/2}Li_{1/2}TiO_3$–$0.06BaZrO_3$ with R-T phase boundary and the temperature stability of d_{33} in $Ba(Zr_{0.2}Ti_{0.8})O_3$–$50(Ba_{0.7}Ca_{0.3})TiO_3$ were considered as the compared samples [40, 51], as shown in Fig. 1.10d. The temperature stability of piezoelectricity can be greatly enhanced in this work by the composition modifications, and high piezoelectricity can be simultaneously shown. In the past of thirteen years, great progresses have been made in the KNN-based materials, including piezoelectricity as well as its stability. More importantly, the physical mechanisms for enhanced electrical properties were also well addressed.

$Bi_{0.5}Na_{0.5}TiO_3$

For $Bi_{0.5}Na_{0.5}TiO_3$ (BNT)-based materials, two kinds of phase boundaries {MPB (I) and MPB (II)} can be often found by doping different additives, where the coexistence of ferroelectric rhombohedral and tetragonal phase boundary was called as MPB (I) and ferroelectric and relaxor pseudocubic phase boundary was denoted

as MPB(II). In the vicinity of MPB (I), the peak piezoelectric constant together with a saturated *P-E* loop can be observed, and a classical sample was shown in BNT-BT materials (Fig. 1.12a) [52]. Even if the MPB (R-T) can be driven, there is still no major breakthrough in the piezoelectricity ($d_{33} \leq 234$ pC/N). More importantly, the d_{33} coming from MPB (I) is strongly dependent on the depolarization temperature (T_d), that is, the d_{33} almost disappears for $T \sim T_d$, which seriously affected the practical applications.

It is well accepted that the MPB (1) can positively enhance the piezoelectric properties of BNT-based materials. Among these alternative MPB compositions, the $(1-x)Bi_{1/2}Na_{1/2}TiO_3$–$xBaTiO_3$ is a classical candidate for the investigation of phase structure. In 1991, T. Takenaka et al. reported the morphotropic phase boundary consisting of rhombohedral (F_α)-tetragonal (F_β) phases in $(1-x)Bi_{1/2}Na_{1/2}TiO_3$–$xBaTiO_3$ ceramics by X-ray diffraction data [52], as shown in Fig. 1.12a. However, an obvious difference in phase diagram was found by combining dielectric characterization and crystal structure analysis with transmission electron microscopy (TEM), as shown in Fig. 1.12b [53]. Some different characteristics for the phase diagram are shown here. First of all, the new phase region for

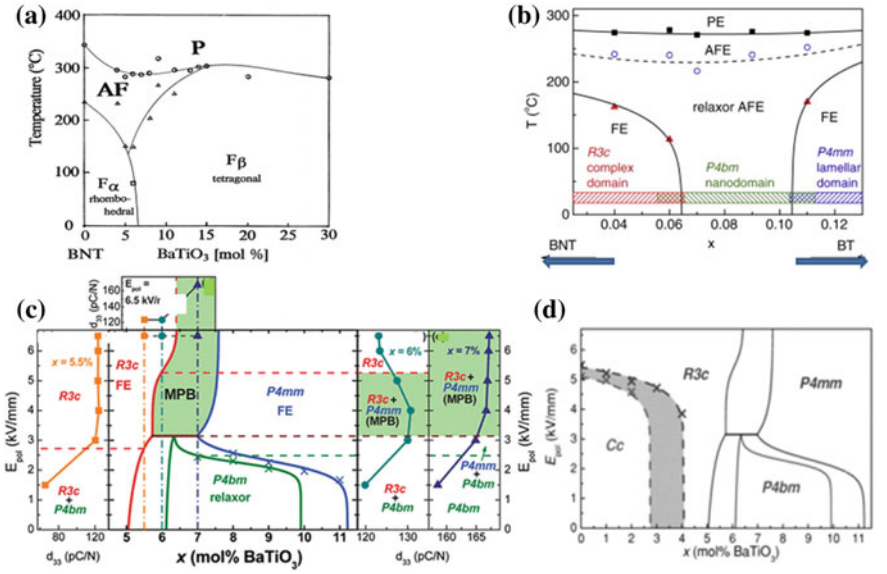

Fig. 1.12 **a** Phase diagram for $(1-x)Bi_{1/2}Na_{1/2}TiO_3$–$xBaTiO_3$ ceramics reported by T. Takenaka et al. [52]. **b** Phase diagram for the unpoled $(1-x)Bi_{1/2}Na_{1/2}TiO_3$–$xBaTiO_3$ ceramics reported by X. L. Tan et al. [53]. **c** Piezoelectric properties versus composition or poling electric field as well as phase diagram for the poling electric field versus x in $(1-x)Bi_{1/2}Na_{1/2}TiO_3$–$xBaTiO_3$ (x = 0.05–0.0115) ceramics [54]. **d** E_{pol} versus x phase diagram of $(1-x)Bi_{1/2}Na_{1/2}TiO_3$–$xBaTiO_3$ (x = 0–0.06) ceramics [55]. Reprinted with permission from Ref. [52]. Copyright © 1991, The Japan Society of Applied Physics. Reprinted with permission from Ref. [53]. Copyright © 2010, Elsevier. Reprinted with permission from Ref. [54]. Copyright © 2012, The American Physical Society. Reprinted with permission from Ref. [55]. Copyright © 2013, Wiley

P4bm symmetry was exhibited between the ferroelectric *R*3*c* and *P*4*mm*. In addition, the ferroelectric domains (>100 nm) with well-defined domain walls was observed in the compositions with $x \leq 0.06$ and $x \geq 0.11$ along with the long-range ferroelectric order at room temperature, and the antiferroelectric nanodomains of the ceramics with $0.07 \leq x \leq 0.09$ can induce the relaxor antiferroelectric behavior. Therefore, it was thought that maximum piezoelectric properties in $(1 - x)$BNT–xBT were obtained at an MPB separating a ferroelectric and a relaxor antiferroelectric phase [53]. In 2012, it was found that the MPB in $(1 - x)$BNT–xBT (x = 5–11.5%) materials can be controlled by the application of electric poling [54], where the real-time evolution of crystal structure and domain morphology during the poling-induced phase transitions can be characterized by in situ TEM. One can see from Fig. 1.12c that the ferroelectric-to-ferroelectric phase transitions during the poling process can completely change the types of MPB. The d_{33} versus poling electric field (E_{pol}) for x = 5.5, 6, and 7% is also shown in Fig. 1.12c [54]. The electric field-induced phase structure can determine the magnitude of piezoelectric properties of this work. For example, d_{33} increases up to 167 pC/N for x = 7% under E_{pol} = 6.5 kV/mm due to the formation of a stable MPB (*R*3*c*/*P*4*mm*) during poling process. The phase diagram for E_{pol} versus x for $(1 - x)$ BNT–xBT (5–11.5%) was used to summarize the phases evolution with poling fields at room temperature. It was found that the MPBs (*R*3*c*/*P*4*bm* and *P*4*bm*/*P*4*mm*) converged with the increase of E_{pol}, and an *R*3*c*/*P*4*mm* was formed with the further increase in E_{pol}. Therefore, the MPB of the ceramics can be destroyed (x = 5.5 and 6%), created (x = 7%) or even replaced by another MPB (x = 6%) during poling. After that, the evolution of phase structures was also identified for the $(1 - x)$BNT–xBT ceramics with $x < 6\%$ [55], as shown in Fig. 1.12d. The phase relationship in the ceramics with $x < 6\%$ was clearly confirmed. The ceramics with x = 3–4% presented a new phase boundary separating the *Cc* and *R*3*c* phases. As shown in Fig. 1.12d, this *Cc*/*R*3*c* phase boundary was curved, indicating that the previously unexplained electric field-induced phase transition in the low-$BaTiO_3$-content compositions belongs to a *Cc*-to-*R*3*c* structural transition [56].

Another new phase boundary between ferroelectric to relaxor pseudocubic phases [MPB(II)] can be observed, which can result in a giant strain property as well as a slimly or pinched *P*-*E* loop. The typical candidate is $0.92Bi_{0.5}Na_{0.5}TiO_3$–$0.06BaTiO_3$–$0.02K_{0.5}Na_{0.5}NbO_3$ (Fig. 1.13a), and then a giant strain value of 0.45% (8 kV/mm) was reported in 2007 [57]. It is the first time to realize such high unipolar strain (0.45%) in polycrystalline lead-free piezoelectric materials, which is comparable with some PZT-based antiferroelectric ceramics. In addition, the large S_{max}/E_{max} of ~560 pm/V can be observed in the ceramics with x = 0.02 (Fig. 1.13c), which is also higher than the reported values of other lead-free and non-textured lead-based polycrystalline ceramics. In 2016, Tan et al. reported a giant electrostrain (~0.70%) and d^*_{33} (~1400 pm/V) in $\{[Bi_{1/2}(Na_{0.84}K_{0.16})_{1/2}]_{0.96}Sr_{0.04}\}(Ti_{1-x}Nb_x)O_3$ (x = 0.025) ceramics because of electric field-induced phase transitions (Fig. 1.13b) [58]. As shown in Fig. 1.13d, the strain properties of

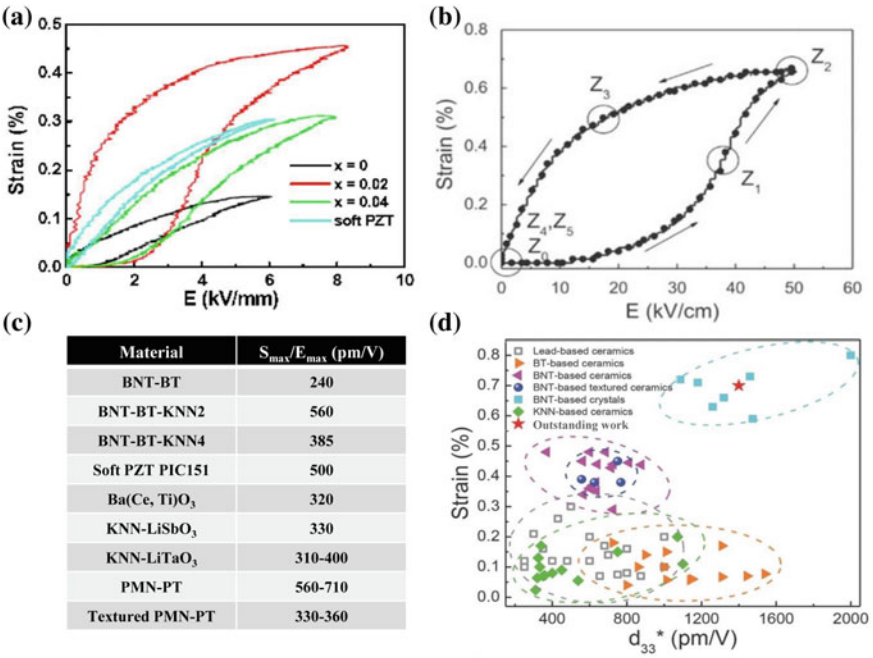

Material	S_{max}/E_{max} (pm/V)
BNT-BT	240
BNT-BT-KNN2	560
BNT-BT-KNN4	385
Soft PZT PIC151	500
Ba(Ce, Ti)O_3	320
KNN-$LiSbO_3$	330
KNN-$LiTaO_3$	310-400
PMN-PT	560-710
Textured PMN-PT	330-360

Fig. 1.13 **a** Unipolar strain of $(0.94–x)Bi_{0.5}Na_{0.5}TiO_3–0.06BaTiO_3–xK_{0.5}Na_{0.5}NbO_3$ ceramics with $x = 0$, 0.02, and 0.04 in comparison to electric field-induced unipolar strain curve of commercial soft PZT [57]. **b** The strain developed in $[Bi_{1/2}(Na_{0.84}K_{0.16})_{1/2}]_{0.96}Sr_{0.04}\}(Ti_{1-x}Nb_x)O_3$ ($x = 0.025$) ceramic under unipolar fields [58]. **c** The comparison of S_{max}/E_{max} of reported data on different materials [57]. **d** Comparison of lead-free solid solution families against their electrostrains and d^*_{33}. Lead-based ceramic oxides are also included for reference. Reprinted with permission from Ref. [57]. Copyright © 2007, AIP Publishing LLC. Reprinted with permission from Ref. [58]. Copyright © 2015, Wiley

BNT-based ceramics are even better than those of some single crystals. More importantly, the strain enhancement can be shown in the vicinity of MPB(II), the peak d^*_{33} can be appeared for $T \sim T_d$, and the strain value still remained even if the measurement temperature is over T_d. As a result, the types of MPB in BNT not only controlled the electrical properties but also changed the temperature stability of the corresponding properties.

1.2.2 Microstructure

The physical properties of a ferro/piezoelectric material can be determined by not only compositions but also microstructure. In the past, several kinds of effective methods have been employed to enhance their physical properties, including the searches for new materials, chemical modification, and the optimization of

microstructure. Here, we discuss the relationship between microstructure and physical properties of a ferro/piezoelectric ceramic.

1.2.2.1 Grain Morphology Versus Electrical Properties

It is well known that the microstructure of ferro/piezoelectric materials can be affected by several factors, such as sintering parameters (e.g., sintering method, sintering aid, sintering atmospheres), chemical composition, preparation techniques, and so on [45, 59–62]. Recently, some typical reports have illustrated that the optimum grain morphologies can be obtained by the variations of sintering parameters [45, 59–65]. First, different sintering methods can change the microstructures of the ceramics [63, 64]. For example, the hot-pressed specimens always exhibit a finer microstructure respecting to the ones by the normal sintering [63], and a high density approaching the theoretical one can be achieved under a lower sintering temperature by spark plasma sintering (SPS) [64]. Secondly, grain morphologies of the ceramics can be optimized by the addition of sintering aids (e.g., CuO, ZnO, MnO, MnO_2 and NiO), which can effectively improve the sintering ability [45, 60]. More importantly, the use of sintering aids can generate some vacancies, which can offset the formation of hygroscopic impure phases in perovskite materials [45, 65]. Thirdly, the sintering atmospheres can affect the grain growth behavior of the ceramics because of the different edge free energies in nucleation steps [45, 60, 62]. It is well known that the denser bulks can be realized due to the existence of liquid or "transient" liquid phase during the sintering process [45, 62], and then the grain growths are also impacted because of the increased atomic mobility [45, 62]. However, the existence of some pores always resists the formation of dense bulks and the grain growth of the ceramics [66]. Typically, some pores can be found in $(1 - x)Bi_{1-y}Sm_yFeO_3$–$xBiScO_3$ ceramics due to the volatilization of Bi_2O_3 and the generation of oxygen vacancies [66]. Therefore, the modification of sintering atmospheres would effectively reduce the concentration of pores. For example, the dense microstructure is revealed in $Pb_{0.91}La_{0.09}(Zr_{0.35}Ti_{0.65})_{0.9775}O_3$ ceramics as the sintering atmosphere changed from air, 33% O_2 to pure O_2 atmosphere [67], and it is also proved that the KNN samples sintered under oxygen atmosphere are denser than sintered in air [68]. Similar phenomenon can be found in the corresponding ferro/piezoelectric thin films or nanostructure [42].

Besides the sintering parameters, chemical composition also plays a crucial role in the grain morphologies of a material. Previous experiments show that the use of different chemical modifications always changes the grain morphologies of the ceramics. For example, the addition of optimum Ca^{2+} would promote the grain growth of KNN or BT-based ceramics [69], and the $SrTiO_3$ always causes the decreased grain sizes of KNN or BNT-based ceramics [70]. In addition, grain morphologies of piezoelectric materials can be well controlled by different preparation techniques [71, 72]. For example, the dense microstructure with homogeneous grains (200–400 nm) is achieved in 0.92BNT–0.08BT ceramics prepared by an acetate-alkoxide sol-gel method [71], while micron order grains of 1 μm are

presented in $0.95Bi_{1/2}Na_{1/2}TiO_3$–$0.05BaTiO_3$ ceramics synthesized by citrate-gel method [72].

For most ferro/piezo-electric ceramics, electrical properties could be partly influenced by the grain morphologies [45, 62]. Typically, the reduced pores may effectively promote the electrical properties of the ceramics due to the involvement of dense microstructure [66]. In addition, the grain sizes also make a positive impact on the electric properties in lead-based or lead-free ceramics [73, 74]. For example, a high d_{33}^* of 279 pm/V can be found in the $0.3Pb(In_{1/2}Nb_{1/2})O_3$–$0.38Pb(Mg_{1/3}Nb_{2/3})O_3$–$0.32PbTiO_3$ ceramics with uniform grains, while a lower d_{33}^* can be observed in the materials with an average size of 2.2 μm [75]. As far as the lead-free piezoceramics are concerned, the grain growth also plays an important role in their electrical behavior [76–78]. For example, a number of large grains partly induce high d_{33} of 276 pC/N in the Li/Ta-modified $(Na,K)NbO_3$ ceramics except for the effect of phase boundaries [76], and pure $BaTiO_3$ ceramics reveal a d_{33} of 290 pC/N due to the involved large grains [77]. Therefore, it is obvious that the grain sizes can change the ferro/piezoelectric properties in the ceramics.

Here, the relationship between microstructure and ferro/piezoelectric properties of piezoelectric ceramics is addressed (Fig. 1.14 and Table 1.1). As shown in Fig. 1.14a and Table 1.1, a large d_{33} of 550 pC/N can be achieved in the PZT-5H ceramics due to globular and large grains of 2.27 μm besides MPB [73]. In addition, a large d_{33} of 490 pC/N can be found in $0.96(K_{0.48}Na_{0.52})Nb_{0.95}Sb_{0.05}O_3$–$0.04Bi_{0.5}(K_{0.18}Na_{0.82})ZrO_3$ ceramics with an average grain size of 1.61 μm and dense microstructure except for R-T (Fig. 1.14b and Table 1.1) [79]. In particular, a larger grain size of ~48 μm can be found in $(Ba_{0.94}Ca_{0.06})(Ti_{0.90}Sn_{0.10})O_3$ ceramics with R-O/O-T, and then a giant d_{33} of ~600 pC/N can be demonstrated

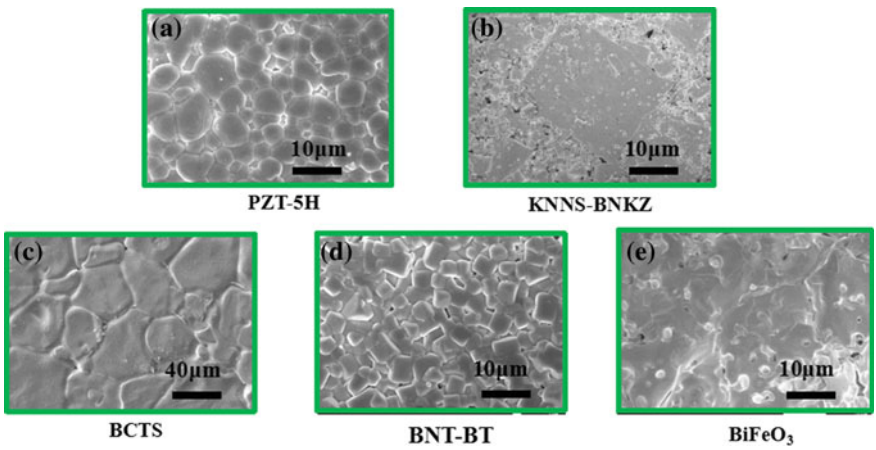

Fig. 1.14 FE-SEM morphologies of **a** PZT-5H, **b** KNNS-BNKZ, **c** BCTS, **d** BNT-BT, and **e** BFO ceramics [66, 73, 79, 80]. Reprinted with permission from Ref. [66]. Copyright © 2015, American Chemical Society. Reprinted with permission from Ref. [73, 79, 80]. Copyright © 2017, 2015 and 2016, Royal Society of Chemistry

Table 1.1 Grain size, phase structure and electrical properties of some typical piezoceramics

Compositions	Grain size (μm)	Phase structure	d_{33} (pC/N)	P_r (μC/cm^2)	Ref
PZT–5H	2.27	R-T	550	38	[73]
$0.96(K_{0.48}Na_{0.52})Nb_{0.95}Sb_{0.05}O_3$–$0.04Bi_{0.5}(K_{0.18}Na_{0.82})ZrO_3$	1.61	R-T	490	13.1	[79]
$0.94(K_{0.5}Na_{0.5})NbO_3$–$0.06LiNbO_3$	8	O-T	215	20	[74]
$BaTiO_3$	8	–	290	14.7	[77]
$(Ba_{0.94}Ca_{0.06})(Ti_{0.90}Sn_{0.10})O_3$	48.54	R-O/O-T	600	14.54	[80]
$Bi_{0.5}(Na_{0.70}K_{0.25}Li_{0.05})_{0.5}TiO_3$	1.9	–	143		[62]
$0.94Bi_{0.5}Na_{0.5}TiO_3$–$0.06BaTiO_3$	1.77	R-T	140	32	[73]

(Fig. 1.14c) [80]. Nevertheless, small grains of 1.77 μm appear in $0.94Bi_{0.5}Na_{0.5}TiO_3$–$0.06BaTiO_3$ ceramics with R-T, and then a d_{33} ($\sim$140 pC/N) is observed (Fig. 1.14d). Interestingly, pure $BiFeO_3$ ceramics with d_{33} ($\sim$51 pC/N) also show large grains (Fig. 1.14e) [66], and however the lack of phase boundaries results in a poor d_{33}. As a result, the modification of grain morphologies is a crucial and indispensable tool to elevate the piezoelectric performance in lead-based and lead-free piezoceramics except for the construction of phase boundaries.

1.2.2.2 Domain Structure Versus Electrical Properties

Domain Types Versus electrical properties

Ferroelectric and related properties in ferroelectric materials are strongly dependent on the domain configurations, and thus the modulation of domain configuration is important for the ferroelectric-related applications, which is called as domain engineering. As we know, domain engineering is one of the most important techniques to realize the property enhancement of ferroelectric materials.

The ferroelectric domain structures of piezoceramics have been widely investigated on the basis of the experimental observations and theoretical analysis [81, 82]. According to the previous investigations, domain switching can change the electrical properties substantially in ferroelectric materials [81, 82]. It is well known that ferroelectric materials possess the domains with uniform polarization along the direction of applied electric fields [81, 82]. Previously, it was reported that both 180° and non-180° domain switching would easily happen in Pb-based materials near MPB. As shown in Table 1.2, the 90° domain walls can be observed in $(1 - x)BiScO_3$–$xPbTiO_3$ ceramics [83], and non-180° domain walls are easily detected in $(1 - x)PbMg_{1/3}Nb_{2/3}O_3$–$xPbTiO_3$ single crystals [84]. For KNN-based ceramics with O-T, the typical domain structures consisting of 60°, 90°, 120° and 180° domain walls are presented [85]. However, non-180° domain wall could